EARTH'S CRYOSPHERE
SCIENTIFIC JOURNAL

Earth's Cryosphere, 2020, vol. XXIV, No. 2, pp. 34–40 **http://earthcryosphere.ru/**

GASES AND GAS HYDRATES IN THE EARTH'S CRYOSPHERE

DOI: 10.21782/EC2541-9994-2020-2(34-40)

INFLUENCE OF HYDRATE FORMATION ON GAS PERMEABILITY VARIATIONS IN FROZEN SANDS

E.M. Chuvilin[1], S.I. Grebenkin[1], D.A. Davletshina[1,2], M.V. Jmaev[2]

[1] *Skolkovo Institute of Science and Technology, Skolkovo Innovation Center, build. 3, Nobil str., Moscow, 143026, Russia; e.chuvilin@skoltech.ru*
[2] *Lomonosov Moscow State University, Faculty of Geology, 1, Leninskie Gory, Moscow, 119991, Russia*

The study of gas permeability variations in frozen sand samples exposed to subfreezing temperatures during hydrate formation included experimental modeling with the experiments run on a specially designed system, which enabled determination of gas permeability of dispersed soils in a context of freezing and hydrate saturation. The experimentally obtained data on gas permeability variations in frozen sand samples artificially saturated with methane or carbon dioxide during hydrate formation at a temperature of −5 °C has revealed that a decrease in gas permeability occurring during hydrate formation in frozen sand samples is controlled primarily by the initial ice content. A reduction in gas permeability depending on the fraction of pore ice converted to hydrate has been calculated. At this, the behavior of reduced gas permeability in frozen sand samples is found to be largely influenced by the type of hydrate-forming agent.

Frozen sands, hydrate formation, gas permeability, ice saturation, gas hydrates, methane, carbon dioxide

INTRODUCTION

Naturally occurring gas hydrates are known to exist under specific pressure and temperature conditions in deep marine environments (ocean-bottom sediments) and in areas with thick permafrost or in the underlying unfrozen sediments (sub-permafrost horizons) [*Istomin, Yakushev, 1992*]. In permafrost settings, a prerequisite for existence of gas hydrates is associated with accumulation of natural gas (primarily, methane) in large amounts in the conditions appropriate for hydrate formation as a result of gas and water freezing in situ in profoundly cooled ground over a long period of time. Numerous gas liberation phenomena which may be directly attributable to dissociating intra-permafrost gas hydrates were reported as early as 1970s during development of numerous oil/gas fields in Western Siberia [*Cherskiy et al., 1983; Ginsburg, Soloviev, 1990; Are, 1998; Yakushev, 2009*].

Formation of permafrost-hosted gas hydrates (in gas-saturated sediments) under conditions allowing for pure methane hydrate to be stable, i.e. origination of gas hydrate stability zone (HSZ), takes place both at low positive and negative temperatures, when a gas accumulation that has not converted to gas hydrate becomes trapped within frozen sediments [*Cherskiy et al., 1983; Ginsburg, Soloviev, 1990; Istomin, Yakushev, 1992; Romanovsky, 1993; Chuvilin et al., 2000*]. In this situation, formation of gas hydrate is based on gas molecule entrapment by ice matrix.

Note that permanently frozen sediments may favor cryogenic concentration of gases and their subsequent accumulation in horizons with good reservoir properties [*Yakushev, 1989, 2009; Chuvilin et al., 2000*]. Further freezing of such "gas pockets" may create above equilibrium pressure, thereby leading to the gas phase change to its hydrate form. In permafrost regions, gas hydrates also form by freezing in closed talik (unfrozen ground) zones saturated with gas, usually localized beneath lakes [*Istomin et al., 2018*]. In addition to cryogenic concentration, the formation of permafrost-associated gas hydrate is favored by the pressure effect (the so called "baric factor") which is associated either with the overlying ice sheets (continental glaciation) or with transgressions of the Arctic seas (when gas and water froze in place during ice-age cooling events) [*Trofimuk et al., 1986; Romanovsky, 1993*]. Thus, glacial ice aggradation atop thick permafrost promotes expansion of the zone of hydrate stability into permafrost, forcing the permafrost table to occur at shallow depths.

Gas hydrates in areas of permafrost distribution are therefore localized beneath permafrost at low positive temperatures, as well within permafrost at negative temperatures, and play a fairly critical role in stability of permafrost environments. The presence of gas hydrates in frozen sediments affects significantly their thermal and mechanical properties, as well as porosity and permeability.

The literature data analysis has revealed only few works investigating thermophysical, mechanical properties and permeability of frozen hydrate-saturated deposits [*Ershov et al., 1996; Chuvilin, Grebenkin, 2015; Li et al., 2016; Chuvilin, Bukhanov, 2017; Chuvilin et al., 2018*]. Studies of porosity and permeability of hydrate-saturated rocks generally investigate these aspects at positive temperatures. However, some of them highlight porosity and permeability of rocks containing either pore ice or pore hydrate [*Ananyan et al., 1972; Starobinets, Murogova, 1985; Seyfried, Murdock, 1997; Jaiswal et al., 2004; Minagawa et al., 2005; Murray et al., 2006; Kneafsey et al., 2008; Kumar et al., 2010; Johnson et al., 2011; Chuvilin, Grebenkin, 2015; Chuvilin et al., 2018*], as well as ice formed during the freezing of hydrate-saturated sediment. Yet, the obtained research results provided extremely scant experimental data on changes in frozen sediment permeability to gas (henceforward, gas permeability) upon hydrate formation from pore ice.

With this in mind, special experiments have been designed and conducted to study gas permeability of frozen sediments during hydrate formation.

EXPERIMENTAL METHODS

Gas permeability variations in hydrate-bearing sands were studied using a method designed by the authors jointly with colleagues from Schlumberger Company [*Chuvilin, Grebenkin, 2015*] by means of gas flushing through a sample on a specially designed experimental setup which allows creating and maintaining pressure and temperature conditions suitable for artificial freezing and hydration of sand samples. The procedure involved: i) preconditioning of soil sample to provide a specified water content, its freezing and saturation of the frozen sample with a hydrate-forming gas in a special pressure cell, ii) hydrate accumulation, iii) testing the sample for permeability to gas at different gas pressures and temperatures, and iv) processing the experimental data.

The experimental study of gas permeability variations in ice- and hydrate-containing sediments employed a system specially designed by EcoGeosProm LLC (Fig. 1), which maintains sample temperatures and pressures widely ranging from −15 to +30 °C and up to 100 bar, respectively.

Preparation of soil sample with prespecified moisture content at the beginning of the experiment included the following steps: air-dried soil mass was thoroughly mixed with water and rested for half an hour for uniform moisture saturation. After that, the moisturized soil was placed in a rubber cuff 3 cm in diameter and compacted layer-by-layer (the length soil of sample is 3–4 cm). Then the sample was placed into the pressure cell, to be exposed to compression (pressure: up to 60 bar) and freezing, with temperature and pressure being monitored in the pressure cell during the run. After that the sample was saturated with a hydrate-forming gas (CH_4 and CO_2) along with the gas permeability monitoring.

The levels of pore filling with hydrate and ice were found using the PVT (pressure–volume–temperature) analysis during the experiment [*Chuvilin et al., 2019*]. The main calculated parameters are described below.

The hydration coefficient (K_h) is the proportion of pore water converted to hydrate relative to total amount of water in the sample, which was found using the formula

$$K_h = \frac{W_h}{W},$$

where W_h is the amount of moisture converted to hydrate (% relative to dry sample weight); W is the moisture content by weight, %.

Percentage of pore filled with hydrate or hydrate saturation (S_h, %):

$$S_h = \frac{H_v}{n},$$

where n is the sample porosity; H_v is the volume content of hydrate, %;

$$H_v = \frac{M_h \rho}{M_s \rho_h} \cdot 100\,\%,$$

where M_h is the mass of pore hydrate, g; M_s is the mass of soil sample, g; ρ is the initial (before hydrate saturation) density of soil, g/cm^3; ρ_h is the density of empty crystalline lattice of methane hydrate equal to 0.794 g/cm^3 [*Chuvilin, Bukhanov, 2017*].

Percentage of pore space filled with ice, or ice saturation (S_i, %) was determined as

$$S_i = \frac{\rho_d W}{0.92n},$$

where ρ_d is density parameter of the soil skeleton.

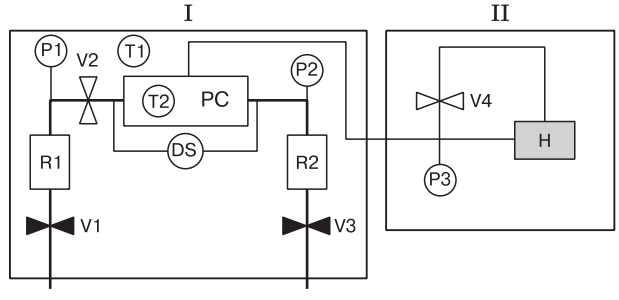

Fig. 1. Schematic map of the experimental setup for evaluating gas permeability in sand samples:

I – measuring system; II – triaxial compression system; V1–V3 = membrane valves for gas input; V4 = ball valve of the hydraulic system; R1, R2 = receivers of gas input; P1–P3= pressure sensors; DS = differential pressure sensor; H = hydraulic pump with an oil tank; PC = pressure cell; T1, T2 = temperature sensors.

The hydrate content values in soils were calculated using the hydrate numbers 5.9 (for CH_4) and 6.1 (for CO_2).

The effective gas permeability (K_g, mD) of the frozen hydrate-containing sand sample was calculated by solving the differential equation of mass transfer through the sample under the pressure gradient [*Chuvilin, Grebenkin, 2015*]:

$$K_g = \frac{2\eta L V_1 p_1 (p_{10} - p_{1k})}{S p_{10} (p_1^2 - p_2^2) t_1},$$

where η is the dynamic viscosity of gas, Pa·s; L is the length of sample, cm; S is the cross-section area of sample, cm^2; V_1 is the receiver volume, cm^3; p_1 is the pressure at sensor 1 (before the sample) at the time t_1 (bar); p_2 is the pressure at sensor 2 (after the sample) at time t_1 (bar); p_{10} is the pressure before the sample at the start time, bar; p_{1k} is the pressure at sensor 1 at the end time, bar.

The relative permeability value (K_r, u.f.) also used in the calculations is determined as the ratio of the effective permeability of the hydrate-saturated sample to the frozen sample permeability at the start of the experiment.

The object of the experimental study were deformed natural sands of marine genesis (mQ_3) recovered while drilling into permafrost (sampling depth: 36–46 m) within the South Tambey gas condensate field (Yamal Peninsula). The particle size distribution of fine-grained sand (according to the E.M. Sergeev's classification) was determined according to GOST 12536-2014 [*State Standard, 2014*]:

Particle size distribution in mass fractions, %	0.2	29.1	62.3	8.4
Particle diameter range, mm	1–0.5	0.5–0.25	0.25–0.1	0.1–0.05

The mineral composition of soil was measured using x-ray diffractometry. Fine-grained sand consisted dominantly of quartz (93.7 %), other minerals contained in the sand were albite (5.1 %) and orthoclase (1.2 %). The density of solid grains of fine sand is 2.69 g/cm^3, its salinity inferred from the chemical analysis of water extract is 0.06 %. The physical characteristics of the test sample determined in accordance with standard procedures of GOST 5180-2015 [*State Standard, 2015*] and SNiP 2.02.04-88 [*Building Code..., 1990*] include: specific surface area of the sand (0.24 m^2/g); prespecified moisture content 8.5–14 %; density of soil skeleton varying from 1.54 to 1.73 g/cm^3 and sample density from 1.73 to 1.91 g/cm^3, while porosity of the soil samples lay within the range of 0.35–0.42 u.f. (Table 1).

Table 1. **Characteristics of sand samples before hydrate saturation**

Sample no.	Moisture content, %	Soil skeleton density, g/cm^3	Density, g/cm^3	Porosity, u.f.
1	8.5	1.69	1.84	0.37
2	9.5	1.72	1.88	0.36
3	10	1.73	1.91	0.35
4	11	1.69	1.87	0.37
5	10	1.57	1.73	0.41
6	10	1.68	1.83	0.39
7	12	1.54	1.73	0.42
8	14	1.63	1.86	0.39

RESULTS AND DISCUSSION

Gas permeability of frozen sand samples before hydrate saturation. The initial gas permeability data of frozen sand samples non-containing hydrate are presented in Table 2. These data allow to infer that the highest gas permeability prior to hydrate saturation (K_g = 23.3 mD) is characteristic of sample 1 with ice saturation of 38 %, and the lowest (K_g = 1.5 mD) – of sample 8 with ice saturation of 62.8 %. It is shown that the gas permeability of frozen samples varies within 15–23 mD as ice saturation of pore space increased from 38 to 50 % in the preconditioned sand samples (Fig. 2).

With further increase in ice saturation (>50 %), gas permeability progressively decreases (because of higher occupancy of pore space by ice), and so does the effective porosity.

Variations in permeability of frozen sand samples during hydrate saturation. After determining the initial gas permeability of sand samples upon their freezing, they were saturated with a hydrate-forming gas (CH_4 or CO_2). The samples were saturated with hydrate at a constant negative temperature (−5 °C) and gas pressure higher than equilibrium pressure (50–60 bar for CH_4 and 25–30 bar for CO_2).

Analysis of the obtained data allowed an inference that when pore ice converts to hydrate, a reduction in the effective permeability of the test samples varies widely within a range of 1.5 to 30 times (Table 3).

The lowest reduction in permeability (less than twice) was shown in sample 2 with a low initial ice saturation (41.6 %). After the sample was saturated with CO_2 hydrate, its gas permeability decreased from 20.6 to 12.66 mD. As much as 32 % of the pore

Table 2. **Initial gas permeability of frozen sand samples (before hydrate saturation)**

Sample no.	S_i, %	K_g, mD
1	38.0	23.3
2	41.6	20.6
3	49.2	21.5
4	50.1	19.6
5	40.5	14.6
6	42.9	21.5
7	51.8	5.7

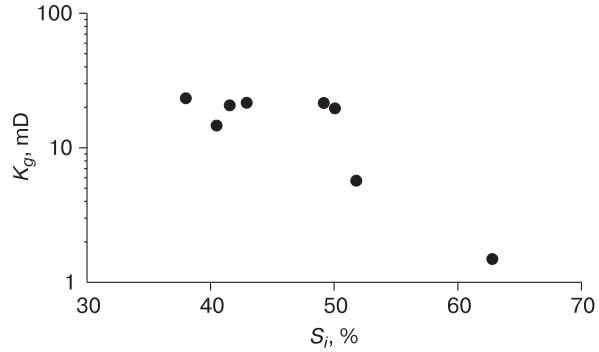

Fig. 2. Ice saturation (S_i) effect on gas permeability (K_g) of frozen sand samples before hydrate saturation at $T = -5$ °C.

Table 3. **Variation in effective gas permeability of sand samples before (numerator) and after (denominator) hydrate saturation at $T = -5$ °C**

Gas	Sample no.	S_i	S_h	$1-(S_i + S_h)$	K_h	K_g
CO_2	1	38.0	0	62.0	0	23.3
		18.5	35.7	45.8	0.62	4.04
	2	41.6	0	58.8	0	20.6
		32.4	23.6	44.0	0.32	12.66
	3	49.2	0	50.8	0	21.5
		35.9	32.4	31.7	0.37	10.44
	4	50.1	0	49.9	0	19.6
		23.5	56.6	19.9	0.64	5.47
CH_4	5	40.5	0	59.5	0	14.6
		21.1	26.6	52.3	0.47	2.04
	6	42.9	0	57.1	0	21.5
		24.1	35.0	40.9	0.59	10.25
	7	51.8	0	48.2	0	5.7
		26.3	54.7	19.0	0.64	0.24
	8	62.8	0	37.2	0	1.5
		51.3	17.9	30.8	0.21	0.05

Note. S_i = ice saturation, %; S_h = hydrate saturation, %; K_h = coefficient of hydration, u.f.; K_g = coefficient of effective gas permeability, mD.

ice was converted to hydrate, with affiliated decrease from 58.8 to 44 % in the fraction of free void pore space ($1 - (S_i + S_h)$).

The permeability values showed the greatest decrease in sample 8 with the maximal (in the experiments) initial ice saturation (62.8 %). When only 21 % of the pore ice was converted to methane hydrate, the sample's permeability decreased by almost 30 times (from 1.5 to 0.05 mD), while the void space changed slightly (from 37.2 to 30.8 %).

The greatest decrease in gas permeability of the frozen sands during hydration is thus observed in samples with a high percentage of pore space filled with ice, despite the fact that the fraction of pore ice changed to hydrate shows a decreasing trend for them.

Analysis of the hydrate formation kinetics revealed that permeability reduction during the pore transition ice to hydrate is marked by certain differentiation between CH_4 and CO_2 hydrate (Fig. 3).

In the test samples saturated with CO_2 hydrate, the ice to hydrate conversion was markedly accelerated. Thus, percentage of ice changed to hydrate over the first 5 hours of the run differed for CO_2-saturated sample 4 (13.9 %) and for methane-saturated sample 6 (about 6 %). During the next day, the rate of ice to hydrate conversion also varied during the first 30 hours of the run: 35 % and 23 % for sample 4 and sample 6, respectively. When hydrate formation rates started to decrease, they became fairly equated: during 50 h after the start of the experiment the percentage of ice changed to hydrate amounted to 43.6 % and 31 % for CO_2- and methane-laden samples, respectively. In later part of the experiment, the ice-to-hydrate conversion rate was lower for carbon dioxide than for methane. Thus, in 120 hours after the start of the experiments, the fractions ice of changed to hydrate accounted accordingly for 58 % in CO_2-laden sample 4 and 52 % and in CH_4-laden sample 6.

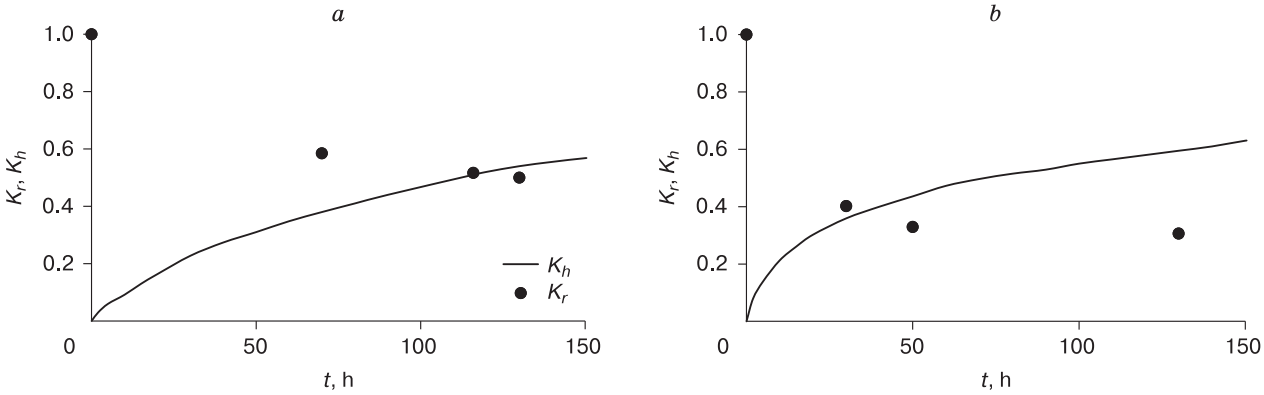

Fig. 3. Time (t)-dependent variations in the hydration coefficient (K_h) and relative gas permeability (K_r) during saturation of sample 6 with CH_4 hydrate (a) and sample 4 with CO_2 hydrate (b).

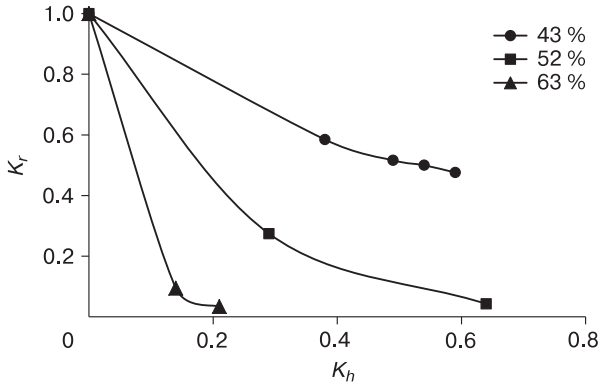

Fig. 4. Effect of the percentage of pore ice converted to methane hydrate (K_h) on the reduction in relative gas permeability (K_r) of frozen sand samples at $T = -5$ °C with different initial ice saturations.

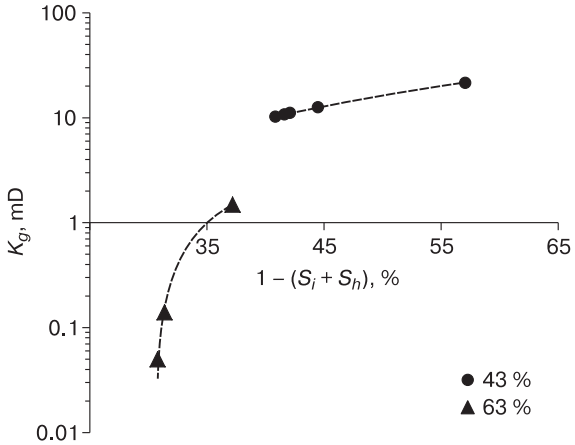

Fig. 5. A relationship between gas permeability (K_g) of frozen sand samples with different initial level of pore filling with ice (43 and 63 %), and variations in void space ($1 - (S_i + S_h)$) during hydrate formation.

All in all, the samples' permeabilities changed inversely proportional to the hydration coefficient throughout the experiment. Despite the greatest decrease in gas permeability was reported in first hours after the hydrate formation for both runs, the permeability behavior differed at a later stage: it changed only slightly with CO_2, and decreased significantly with methane.

Thus, the process of CO_2 hydrate formation from ice occurred more intensely at the start of hydrate formation and slowed down considerably after 50 % of ice converted to hydrate. At this, ice converts to methane hydrate with a lower reduction in the hydrate formation rate over time.

The study enabled analysis of the hydration coefficient (K_h) effect on reduction in gas permeability at

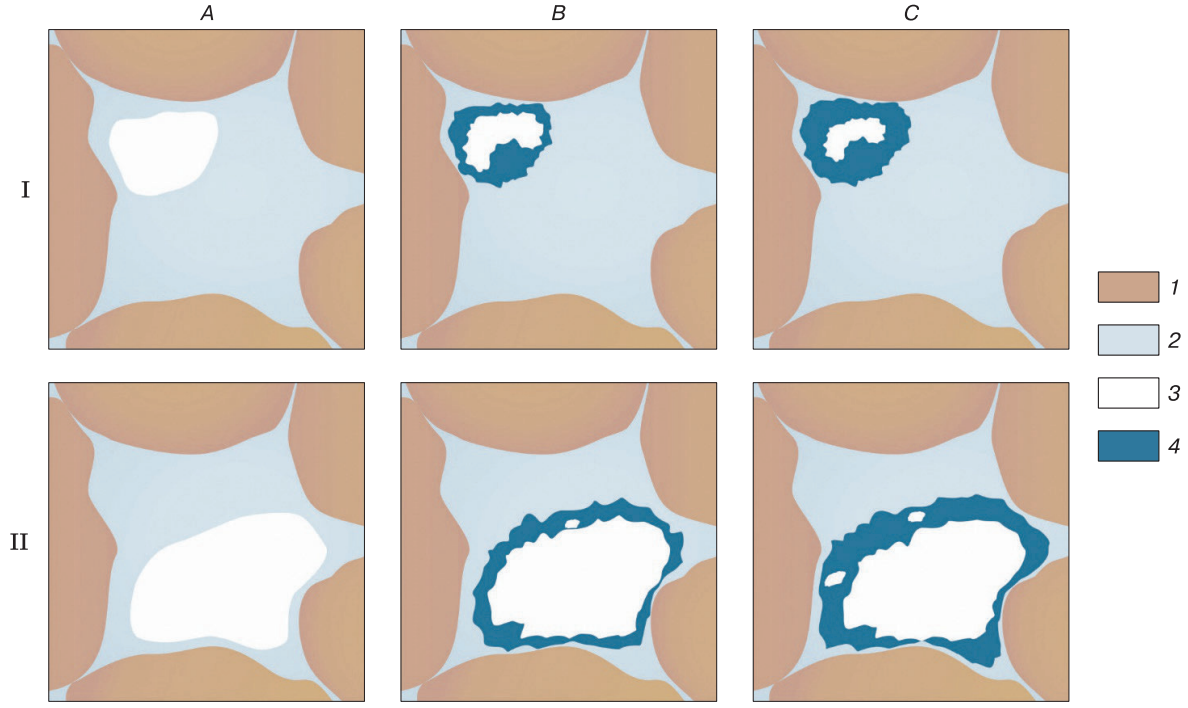

Fig. 6. Schematic diagram of variations in the level of void pore space of gas-saturated frozen sand at high (I) and low (II) percentage of pore space filled with ice during hydrate formation.

A, *B*, *C* – before (*A*), at the start (*B*) and after (*C*) hydrate formation; *1* – sand particles; *2* – ice; *3* – gas; *4* – gas hydrate.

a negative temperature (−5 °C) for all the test samples (Fig. 4).

The results have demonstrated that the higher the initial ice saturation of test samples, the greater the influence of the hydration coefficient on gas permeability, while the maximum reduction in permeability is reported at early stage of the hydrate formation process. Given percentage of pore space filled with ice reduces, the behavior of change in permeability during the pore ice to hydrate conversion shows a smoother pattern.

The effect of hydrate formation process on variations in the void pore space of the sand samples considering their initial percentage of pore space filling with ice differ (43 and 63 %) is shown in Fig. 5.

The calculations demonstrate that during the pore ice to hydrate conversion, the cumulative percentage of pore space filled with ice and hydrate increases due to the difference in their specific volume (about 15 %). Hence, the void pore space will decrease. With higher occupancy of pore space with ice (63 %), even slight changes in void pore space cause a dramatic decrease in the sample's gas permeability, as compared to lower initial ice saturation (43 %) (Fig. 5). A schematic representation of the variations in void pore space of gas-saturated frozen sand at different levels of pore occupancy with ice is shown in Fig. 6.

Thus, changing void pore space during the pore ice to hydrate conversion is interpreted to be one of the major controls of variations in gas permeability of frozen sand samples during hydrate formation.

CONCLUSIONS

An experimental evaluation of the influence of the hydrate formation process on the effective gas permeability of frozen sand samples was carried out. This allowed to infer that hydrate formation at negative temperatures entails a decrease in the gas permeability of ice-containing sand samples. At this, the magnitude of the gas permeability reduction is dictated by the initial ice content. Thus, for a sample with a high cumulative occupancy of pore space with ice (about 63 %), the gas permeability showed a 30-fold decrease, while in the sample with a lower initial ice saturation (42 %), it decreased by less than twice. The experimental studies have highlighted the effect of the type of hydrate-forming gas (CH_4, CO_2), which is primarily manifested through the hydrate formation kinetics and the intensity of gas permeability reduction over time. The gas permeability variation in frozen sand samples is shown to be inversely proportional to the coefficient of hydration.

The work was financially supported by the Russian Foundation for Basic Research (project No. 17-05-00995) and the Russian Science Foundation (grant No. 18-77-10063).

References

Ananyan, A.A., Arutyunyan, N.A., Mazurov, V.A., Silvestrov, L.K., 1972. On permeability of permafrost. Merzlotnue Issledovaniya (Permafrost Studies), No. 12, 205–209.

Are, F.E., 1998. Problem of deep gas emission into the atmosphere. Kriosfera Zemli (Earth's Cryosphere), II (4), 42–50.

Building Codes and Regulations, 1990. SNiP 2.02.04-88. Foundation Beds and Foundations in Permafrost Soils. Gosstroy (USSR), Moscow, 52 pp. (in Russian).

Cherskiy, N.V., Tsarev, V.P., Nikitin, S.P., 1983. Conditions for Gas Accumulation in Gas Hydrate Deposits: Investigation and Prediction. Izd. Yakut. fil. SO AN SSSR, Yakutsk, 156 pp. (in Russian).

Chuvilin, E.M., Bukhanov, B.A., 2017. Effect of hydrate formation conditions on thermal conductivity of gas-saturated sediments. Energy and Fuels, No. 31, 5246–5254.

Chuvilin, E.M., Bukhanov, B.A., Grebenkin, S.I., et al., 2018. Shear strength of frozen sand with dissociating pore methane hydrate: An experimental study. Cold Regions Sci. and Technol. 153, 101–105.

Chuvilin, E.M., Davletshina, D.A., Lupachik, M.V., 2019. Hydrate formation in frozen and thawing methane-saturated sediments. Earth's Cryosphere XXIII (2), 42–52.

Chuvilin, E.M., Grebenkin, S.I., 2015. Gas permeability variations in gas-fi lled soils upon hydrate formation and freezing: an experimental study. Earth's Cryosphere XIX (2), 59–64.

Chuvilin, E.M., Yakushev, V.S., Perlova, E.V., 1998. Gas and gas hydrates in the permafrost of Bovanenkovo gas field, Yamal Peninsula, West Siberia. Polarforschung (erschienen 2000), vol. 68, 215–219.

Ershov, E.D., Yakushev, V.S., Chuvilin, E.M., 1996. Laboratory studies of frozen natural and artificial hydrate-containing rock samples. In: Proc. 2nd Intern. Conf. on Natural Gas Hydrates (Toulouse, France, June 2–6, 1996), Toulouse, pp. 609–615.

Istomin, V.A., Chuvilin, E.M., Sergeeva, D.V., et al., 2018. Thermodynamic calculation of freezing temperature of gas-saturated pore water in talik zones. In: 5th European Conf. on Permafrost (Chamonix, France, June 23–July 1, 2018), Chamonix, pp. 480–481.

Istomin, V.A., Yakushev, V.S., 1992. Naturally Occurring Gas Hydrates. Nedra, Moscow, 235 pp. (in Russian).

Ginsburg, G.D., Soloviev, V.A., 1990. Geological models of gas hydrate formation. Litologiya i Poleznye Iskopaemye (Lithology and Mineral Resources), No. 2, 76–87.

Jaiswal, N.J., Westervelt, J.V., Patil, S.L., et al., 2004. Phase behavior and relative permeability of gas-water-hydrate system. In: Aapg. Hedberg. Conf. "Gas Hydrates: Energy Resource Potential and Associated Geologic Hazards" (Vancouver, BC, Canada, Sept. 12–16, 2004), Vancouver, pp. 26–35.

Johnson, A., Patil, S., Dandekar, A., 2011. Experimental investigation of gas-water relative permeability for gas-hydrate-bearing sediments from the Mount Elbert Gas Hydrate Stratigraphic Test Well, Alaska North Slope. Marine and Petroleum Geol., No. 23, 419–426.

Kneafsey, T.J., Gupta, A., Seol, Y., Tomutsa, L., 2008. Permeability of laboratory-formed methane hydrate-bearing sand, OTC19536-PP, SPE. In: Offshore Technology Conf. (Houston, TX, USA, May 7, 2008), Houston, pp. 21–34.

Kumar, A., Maini, B., Bishnoi, P.R., et al., 2010. Experimental determination of permeability in the presence of hydrates and its effect on the dissociation characteristics of gas hyd-

rates in porous media. J. Petroleum Sci. and Eng., No. 70, 114–122.

Li, Y., Liu ,W., Zhu, Y., et al., 2016. Mechanical behaviors of permafrost-associated methane hydrate-bearing sediments under different mining methods. Appl. Energy 162, 1627–1632.

Minagawa, H., Ohmura, R., Takahashi, T., et al., 2005. Water permeability measurements of natural gas hydrate-bearing sediments obtained from Mallik 5L-38. In: Abstr. of Mallik Intern. Symposium – from Mallik to the Future. Technol. Res. Center Jap. National Oil Corporation, pp. 398–401.

Murray, D., Fukuhara, M., Khong, C.K., et al., 2006. Permeability estimates in gas hydrate reservoirs of the Nankai trough. In: SPWLA 47th Ann. Logging Symposium (Veracruz, June 4–7, 2006), Veracruz, Mexico, pp. 1–6.

Romanovsky, N.N., 1993. Fundamentals of Cryogenesis in the Lithosphere. Moscow University Press, Moscow, 336 pp. (in Russian).

Seyfried, M.S., Murdock, M.D., 1997. Use of air permeability to estimate infiltrability of frozen soil. J. Hydrology 202, 95–107.

Starobinets, I.S., Murogova, R.N., 1985. Screen and conductive role of permafrost in respect to migrating hydrocarbons. Geologiya Nefti i Gaza (Oil and Gas Geology), No. 1, 24–27.

State Standard, 2014. GOST 12536-2014. Soils. Methods of Laboratory Analysis of Granulometric (grain-size) and Microaggregate Distribution. Standards Publishing, Moscow, 24 pp. (in Russian).

State Standard, 2015. GOST 5180-2015. Soils. Laboratory Methods for Determination of Physical Characteristics. Standartinform, Moscow, 23 pp. (in Russian).

Trofimuk, A.A., Makogon, Yu.F., Yakushev, V.S., 1986. Influence of hydrate formation zones on the temperature regime of rocks in permafrost. Geologiya i Geofizika (Soviet Geology and Geophysics), No. 11, 3–10.

Yakushev, V.S., 1989. One possible cause of gas bursts in permafrost. Geologiya Nefti i Gaza (Oil and Gas Geology), No. 14, 45–46.

Yakushev, V.S., 2009. Natural Gas and Gas Hydrates in Permafrost. VNIIGAZ, Moscow, 192 pp. (in Russian).

Received July 4, 2019
Revised version received September 21, 2019
Accepted October 1, 2019